Chapter 10

Förster Resonance Energy Transfer as a Tool for Quantification of Protein–Lipid Selectivity

Luís M.S. Loura, Manuel Prieto, and Fábio Fernandes

Abstract

This chapter addresses the determination of protein–lipid selectivity, here described as the preference of a protein for having a specific type of lipid in its vicinity (annular lipids), from Förster resonance energy transfer methodologies. These allow a quantification of the effect, i.e., the determination of the biasing in distribution of the lipid under study around the protein, as compared to its bulk membrane distribution, with advantages over established approaches that have been used for the same purpose, such as electron spin resonance spectroscopy. The experiment can be carried out with steady-state instrumentation, the formalisms are described in detail, and the model can be applied to a membrane protein of any size.

Key words: Fluorescence, FRET, Lipid/protein interaction, Membrane protein, Protein/lipid selectivity

1. Introduction

1.1. Protein–Lipid Selectivity

Membrane proteins are strongly influenced by the lipidic composition of the protein–lipid interface. Lipids with different charge, hydrophobic thickness, and inherent curvature can drastically promote or reduce protein activity (1, 2). Proteins exhibit preferential interactions with selected lipids, generating a driving force for the creation of lateral lipid heterogeneities in the membrane and these can potentially extend to several lipid shells around the protein. Several peripheral proteins reversibly interact with the membrane after binding to specific lipids, and temporal as well as spatial regulation of these events has been shown to be crucial for several biological functions, including signaling cascades (3).

On the other hand, hydrophobic matching constraints at the transmembrane protein–lipid interface induce enrichment of specific lipids around the protein. Enrichment occurs for lipids that upon interaction with the protein effectively prevent the exposure of hydrophobic protein residues and of the lipid hydrophobic

Jörg H. Kleinschmidt (ed.), *Lipid-Protein Interactions: Methods and Protocols*, Methods in Molecular Biology, vol. 974,
DOI 10.1007/978-1-62703-275-9_10,

groups to the polar aqueous environment. The lipids in direct contact with the transmembrane protein surface embedded in the bilayer are known as annular lipids and typically display fast on–off rates for protein interaction. In some cases, proteins display hydrophobic pockets that correspond to binding sites with higher affinity for specific lipids. Binding of lipids to these sites is often essential for protein activity (4). Protein–lipid selectivity problems are commonly addressed by electron spin resonance (ESR) and fluorescence quenching methods. The former can discriminate between immobilized lipids in contact with the protein and mobile lipids away from the protein interface (5), while the latter relies on the measurement of fluorescence static or collisional quenching induced by contact between the protein and the lipid for a fluorophore in one of the molecules (6, 7). These techniques detect direct contact between protein and lipids but are insensitive to the creation of lateral lipid heterogeneities away from the protein–lipid interface. On the other hand, Förster resonance energy transfer (FRET) is sensitive to distances from 1 to 10 nm and is able to detect both direct binding and deviations from homogeneity of lipid distribution around the protein.

Additionally, FRET sensitivity, like all fluorescence methodologies, is unmatched by other spectroscopic techniques, and lower amounts of membrane proteins are necessary, and there is no restriction on the temperature range to carry out the experiment. Since membrane protein expression and/or purification can be challenging in some cases (particularly for integral proteins), the possibility of conducting experiments with low concentrations of materials is highly useful. Also, a large variety of fluorescent-labeled lipids with different structural features is commercially available allowing for great flexibility in the design of experiments. For these reasons, FRET is an excellent tool for protein–lipid selectivity studies. Here, we present an approach to the quantification of protein–lipid selectivity through FRET that has been successfully applied to different systems.

1.2. Characterization of Protein/Lipid Selectivity by FRET

FRET is a photophysical process by which an electronically excited fluorophore, the donor (D), is quenched by a nearby chromophore, termed acceptor (A), which in turn becomes excited. FRET does not involve molecular contact between the intervening species, but depends acutely on the D–A separation distance, d. Its rate constant for a single D–A pair, k_T, is given by (8)

$$k_T = \frac{1}{\tau_0}\left(\frac{R_0}{d}\right)^6, \tag{1}$$

where τ_0 is the fluorescence lifetime of D in absence of A, and R_0, the so-called Förster radius, is defined as the D–A distance for which k_T is half of the decay rate constant of D in absence of A (given by τ_0^{-1}).

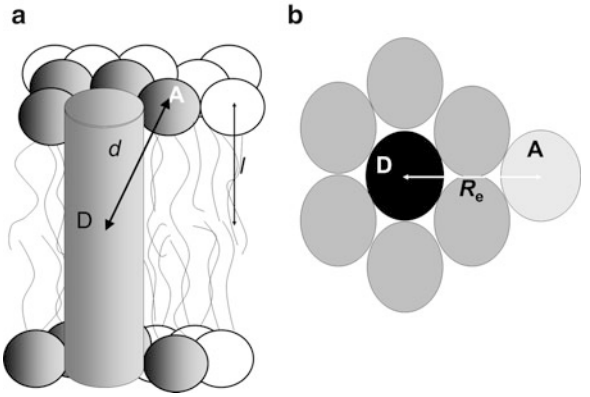

Fig. 1. Molecular model for the FRET analysis according to the model of Fernandes et al. (2004): (**a**) *side view* and (**b**) *top view*. In the model, protein–lipid organization presents a hexagonal geometry. The T36C mutant of M13 MCP was labeled with the FRET donor (coumarin) so that the fluorophore locates in the center of the bilayer, whereas the acceptors are distributed in the bilayer surface. Two different environments are available for the labeled lipids (acceptors): the annular shell surrounding the protein and the bulk lipid. Reprinted with permission from (10). Copyright 2004 Biophysical Society.

R_0 (typically in the 1–6 nm range) is a very important parameter as it measures the range of effective FRET interaction for a given pair. It can be calculated from spectral data, such as D's fluorescence quantum yield (Φ_D) and normalized emission spectrum ($I(\lambda)$) and A's molar absorption spectrum ($\varepsilon(\lambda)$), using the following equation (which assumes nm units for both λ and R_0):

$$R_0 = 0.02108\left[\kappa^2 \Phi_D n^{-4} \int_0^\infty I(\lambda)\varepsilon(\lambda)\lambda^4 d\lambda\right]^{1/6}. \qquad (2)$$

The other parameters needed for this purpose are the orientation factor κ^2 (see (9) for a detailed discussion) and the refractive index n. Experimentally, FRET is usually quantified by the FRET efficiency, E:

$$E = 1 - \tau/\tau_0 = 1 - I_{DA}/I_{D'} \qquad (3)$$

where τ is the lifetime of D in the presence of A, and I_{DA}/I_D is the ratio between the steady-state fluorescence intensity of D in the presence (DA) and absence (D) of A.

Let us consider a membrane protein with approximate cylindrical symmetry, containing a D chromophore (Trp residue or extrinsic covalently attached label) in an axial position, at a given transverse distance. The protein is inserted in a bilayer composed of a single-component host lipid matrix and a small amount of an A lipid probe, surrounded by an annular layer of N closest lipid neighbors (Fig. 1a). N is ~12 (6 in each leaflet) for a protein with a single transmembrane (TM) segment (Fig. 1b) and obviously larger for proteins with multiple TM segments. Each annular site

may be occupied by a host lipid or an A probe molecule. In the latter case, this A molecule acts as potential quencher of D's emission by FRET. The rate constant for this interaction is given by Eq. 1, with d easily calculated, once estimates for average transverse distance between the D and A planes (l) and the lateral separation between both D and A inside the transmembrane protein-annular shell lipids complex (R) are known:

$$d_i = \left(l_i^2 + R^2\right)^{1/2}. \tag{4}$$

In this equation, $i = 1,2$ denotes the possibility that D might not be located in the bilayer midplane, implying that there may be two distinct D–A interplanar distances l_i (and hence two distinct d_i values, and two corresponding k_{Ti} rate constants): one for A lipid probe molecules located on the top bilayer leaflet and another for those on the bottom leaflet. To compute the FRET contribution of annular A molecules to the decay of D, it is assumed that multiple acceptors (or none at all) may occupy the N available sites ($N/2$ in each leaflet), following a binomial distribution. This is done using the following equation (10):

$$\rho_{annular}(t) = \rho_{annular,1}(t)\rho_{annular,2}(t), \tag{5}$$

where

$$\rho_{annular,i} = \sum_{n=0}^{N/2} e^{-nk_{Ti}t}\binom{N/2}{n}\mu^n(1-\mu)^{N/2-n}. \tag{6}$$

μ represents the probability of each of the 12 annular sites to be occupied by an A molecule. It depends on the acceptor molar fraction and on a relative selectivity constant (K_S) which quantifies the relative affinity of the labeled and unlabeled phospholipids (whose concentrations are denoted below by [A] and [L], respectively):

$$\mu = K_S\frac{[A]}{[A]+[L]}. \tag{7}$$

Obviously, not all A molecules are located in the annular region. Some of them will be scattered in the bilayer, assumedly in a uniform distribution. The contribution of these A molecules can be calculated using the analytical solution for FRET in an infinite planar geometry (11, 12):

$$\rho_{ramdom}(t) = \exp\left(-\frac{t}{\tau_0}\right)\prod_{i=1}^{2}\exp\left\{-\pi R_0^2 n_2\gamma\left[\frac{2}{3},\left(\frac{R_0}{R_{ei}}\right)^6\left(\frac{t}{\tau_0}\right)\right]\left(\frac{t}{\tau_0}\right)^{1/3}\right\}\cdot \exp\left\{\pi R_{ei}^2 n_2\left(1-\exp\left[-\left(\frac{R_0}{R_{ei}}\right)^6\left(\frac{t}{\tau_0}\right)\right]\right)\right\}. \tag{8}$$

In this equation, γ is the incomplete gamma function, R_{ei} is the minimum distance (exclusion distance, Fig. 1b) between D and A molecules in leaflet i, and n_2 is the numerical concentration of A (molecules of each bilayer leaflet/unit area = total A molecules/unit area). The value n_2 must be corrected for the presence of labeled lipid in the annular region, which therefore is not part of the randomly distributed acceptors pool.

The overall D decay in presence of A ($i_{DA}(t)$) is now simply computed by multiplying that in absence of A ($i_D(t)$) by the annular and non-annular FRET contributions:

$$i_{DA}(t) = i_D(t)\rho_{annular}(t)\rho_{ramdom}(t). \tag{9}$$

From $i_{DA}(t)$ and $i_D(t)$, E can be computed according to

$$E = 1 - \int_0^\infty i_{DA}(t)dt \Big/ \int_0^\infty i_D(t)dt. \tag{10}$$

This allows comparison of experimental E values (Eq. 3) with theoretical expectations (Eq. 10), as well as retrieval of the model-fitting parameter values (K_S or μ), as illustrated below for the problem at hand.

2. Materials

1. Buffer I: 50 mM sodium cholate, 150 mM NaCl, 10 mM Tris–HCl, 1 mM EDTA, pH 8.
2. Buffer II: 150 mM NaCl, 10 mM Tris–HCl, 1 mM EDTA, pH 8.
3. Buffer III: 20 mM HEPES, 150 mM NaCl buffer, 0.008 % *N*-dodecyl-β-D-maltoside (DDM), pH 7.4.
4. Purified proteins containing D fluorophore: will vary according to the particular system under study. In the examples described in more detail below, these are the T36C mutant of the M13 major coat (purified from M13 bacteriophage and labeled with DCIA fluorophore (7-diethylamino-3((4′iodoacetyl)amino) phenyl-4-methylcoumarin), hereby named DCIA-M13 mcp (10, 13), and lactose permease (LacY) from *Escherichia coli*, which possesses a single tryptophan residue (Trp151) (14). DCIA-M13 mcp was stored in buffer I, while LacY was kept in buffer III.
5. Nonfluorescent lipids: will vary according to the particular system under study. In the examples described in more detail below, these are 1,2-dioleoyl-*sn*-glycero-3-phosphocholine (DOPC), 1,2-dierucoyl-*sn*-glycero-3-phosphocholine (DEuPC), and

1,2-dimyristoleoyl-*sn*-glycero-3-phosphocholine (DMoPC) for the DCIA-M13 mcp system and 1-palmitoyl-2-oleoyl-*sn*-glycero-3-phosphoethanolamine (POPE), 1-palmitoyl-2-oleoyl-*sn*-gly cero-3-phosphoglycerol (POPG), 1,2-dioleoyl-*sn*-gly cero-3-phosphoethanolamine (DOPE), 1,2-dipalmitoyl-*sn*-glycero-3-phosphoethanolamine (DPPE), 1′,3′-bis[1,2-dimyristoyl-*sn*-glycero-3-phospho]-*sn*-glycerol (myristoyl-CL), and 1′,3′-bis[1,2-dioleoyl-*sn*-glycero-3-phospho]-*sn*-glycerol (oleoyl-CL) for the LacY system. Prepare stock solutions in chloroform–methanol mixture (3:1, vol./vol.) and store at −20°C.

6. Lipids with linked A fluorophore: will vary according to the particular system under study. In the examples described inmore detail below, these are 1,2-dioleoyl-*sn*-glycero-3-phosphoethanolamine-*N*-(7-nitro-2-1,3-benzoxadiazol-4-yl) (*N*-NBD-DOPE), 1-oleoyl-2-[12-[(7-nitro-2-1,3-benzoxadiazol-4-yl)amino]dodecanoyl]-*sn*-glycero-Phosphocholine (NBD-PC), 1-oleoyl-2-[12-[(7-nitro-2-1,3-benzoxadiazol-4-yl)amino]dodecanoyl]-*sn*-Glycero-Phosphoethanolamine (NBD-PE), 1-oleoyl-2-[12-[(7-nitro-2-1,3-benzoxadiazol-4-yl)amino]dodeca noyl]-*sn*-glycero-phosphoserine (NBD-PS) (sodium salt), 1-oleoyl-2-[12-[(7-nitro-2-1,3-benzoxadiazol-4-yl)amino] dodecanoyl]-*sn*-glycero-phosphate (NBD-PA) (monosodium salt), and 1-oleoyl-2-[12-[(7-nitro-2-1,3-benzoxadiazol-4-yl)amino]dodecanoyl]-*sn*-glycero-3-[phospho-*rac*-(1-glycerol)] (NBD-PG) (sodium salt) for the DCIA-M13 mcp system, and 1-hexadecanoyl-2-(1-pyrenedecanoyl)-*sn*-glycero-3-phosphoglycerol ammonium salt (Pyr-PG) and 1-hexadecanoyl-2-(1-pyrenedecanoyl)-*sn*-glycero-3-phosphoethanolamine ammonium salt (Pyr-PE) for the LacY system. Prepare stock solutions in chloroform–methanol mixture (3:1, vol./vol.) and store at −20 °C.
7. Spectra/Por CE dialysis membrane (Spectrum Laboratories, Rancho Dominguez, CA) or polystyrene Bio-Beads SM-2, from Bio-Rad (Hercules, CA).

3. Methods

1. Mix adequate volumes of nonfluorescent lipids' stock solutions to prepare 1–10 μmol of total lipid in the desired proportion (see Note 1), to prepare samples without A (D samples).
2. Repeat previous step, also adding an adequate volume of fluorescent lipid stock solution (see Note 2), to prepare samples.
3. After thorough mixing of each sample, dry all samples under a gentle stream of nitrogen until complete evaporation.
4. Dry all samples further by leaving them in vacuum for 6 h.

5. Suspend the dried lipid film in buffer. In the described examples, buffer I is used for the DCIA-M13 mcp system, and buffer III for the LacY system. Liposomes may be extruded or sonicated at this stage to produce unilamellar vesicles.
6. Reconstitute the proteins in the lipid vesicles, in an adequate proportion to yield the desired protein/lipid ratio, which should be the same for all samples of a given system. The exact procedure will depend on the system under study (see Note 3).
7. Measure fluorescence of both D and DA samples. Either a time-resolved or a steady-state fluorescence setup may be used, depending on availability (see Note 4).
8. Calculate experimental FRET efficiencies, E, using Eq. 3 either with the steady-state fluorescence intensities I_D and I_{DA} for a steady-state setup or the lifetimes τ_D and τ_{DA} for a time-resolved setup (see Note 5).
9. If unknown, calculate the Förster distance, R_0, for the D/A pair in study, using Eq. 2. For this purpose, the D emission spectrum and the A absorption spectrum are required, as well as the fluorescence quantum yield of D. Integration is straightforwardly carried out in a spreadsheet, using the rectangle, trapezoidal, or Simpson rules (see Note 6).
10. Fit the model described in Subheading 2 to the experimental FRET efficiencies. For optimal fitting, inputs for all structural parameters (number N of annular sites, areas/host lipid molecule, interplanar distances) should be provided, as well as the R_0 value computed in the preceding step, so that only selectivity parameters are optimized (see Note 7). If a single A concentration is used, this simply equates to determining the value of the μ parameter that matches the experimental and theoretical FRET efficiencies, from which K_s may be calculated using Eq. 7. If (preferably) multiple A concentrations are used, then μ varies for each data point, but is determined by the acceptor mole fraction and the value of the selectivity constant, K_s. The latter is the sole fitting parameter in this case. The whole procedure may be carried out in a (large) spreadsheet (see Note 8).

FRET efficiencies obtained between DCIA-M13 mcp and NBD-labeled lipids are presented in Fig. 2 and Table 1. In order to determine selectivity of M13 mcp for particular phospholipid classes, PE, PC, PG, PS, and PA phospholipids labeled with NBD at the acyl chain were incorporated in proteoliposomes composed of DOPC. M13-mcp exhibits preferential interaction with anionic lipids, particularly for PA and PS. The protein presents a higher affinity for the labeled lipid than for the bulk lipid ($K_S > 1$), possibly as a result of electrostatic interactions with the NBD group. Different K_S values were also recovered for N-NBD-DOPE depending on the thickness of the proteoliposome

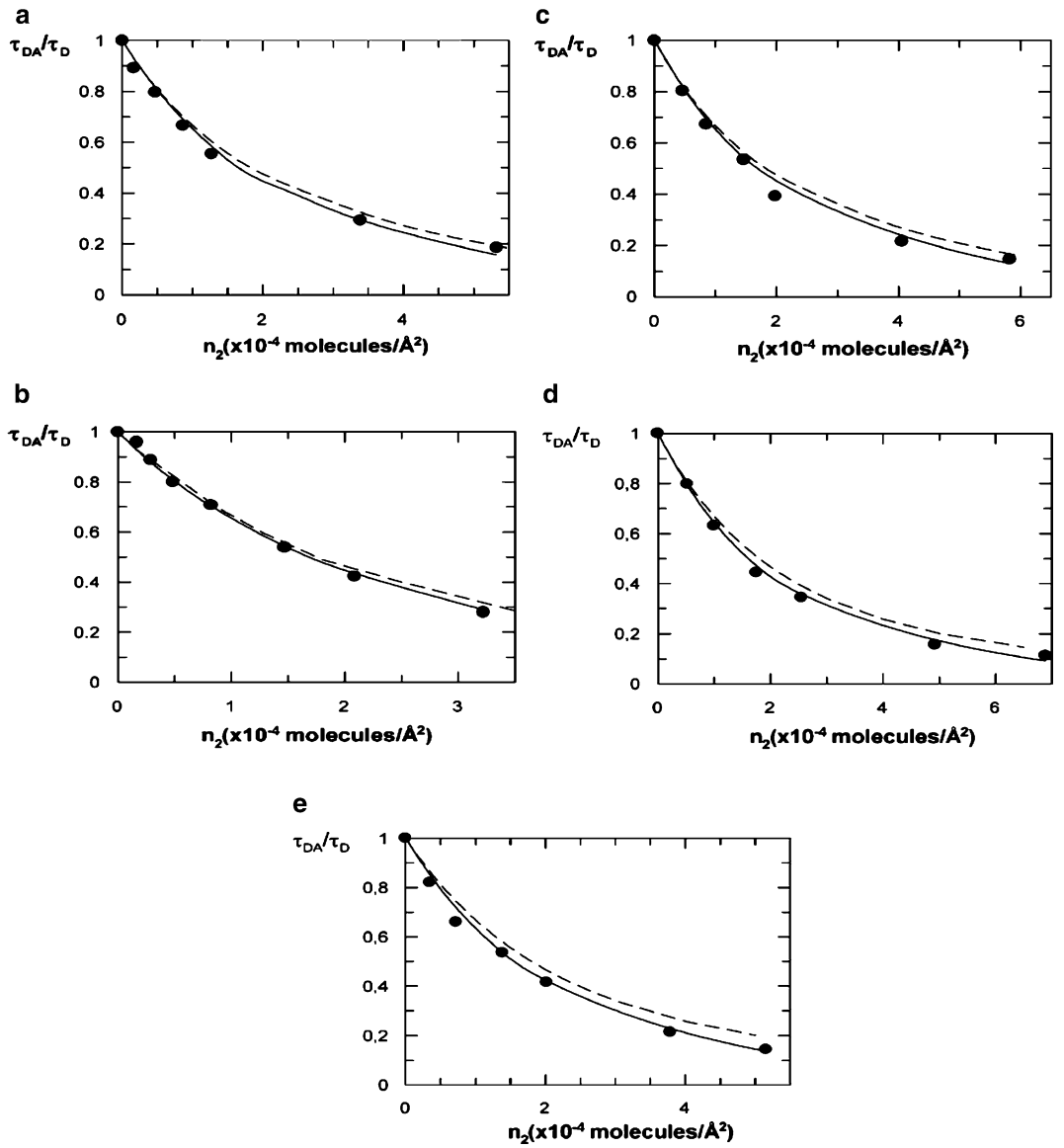

Fig. 2. Donor (coumarin-labeled protein) fluorescence quenching by energy transfer acceptor (18:1-(12:0-NBD)-PX, where X stands for the different headgroup structures) in pure DOPC bilayers. (*filled circle*) Experimental energy transfer efficiencies; (*solid line*) theoretical simulations obtained from the annular model for protein–lipid interaction using the fitted K_S; and (*dotted line*) simulations for random distribution of acceptors ($K_S = 1.0$). (**a**) PC-labeled phospholipid (fitted $K_S = 2.0$); (**b**) PE-labeled phospholipid (fitted $K_S = 2.0$); (**c**) PG-labeled phospholipid (fitted $K_S = 2.3$); (**d**) PS-labeled phospholipid (fitted $K_S = 2.7$); and (**e**) PA-labeled phospholipid (fitted $K_S = 3$). Reprinted with permission from (10). Copyright 2004 Biophysical Society.

membrane (Table 1). M13 mcp is shown to have an increased affinity for *N*-NBD-DOPE when there was considerable mismatch (both positive and negative) between the protein and the bulk lipid, reflecting an enrichment of the hydrophobically matching lipid in the protein interface.

Table 1
Labeled phospholipid relative association constants toward M13 major coat protein

Labeled phospholipid	Bilayer composition	K_S	$K_S/K_S(PC)$[a]
N-DOPE-NBD	di(18:1)PC	1.4	–
N-DOPE-NBD	di(22:1)PC	2.1	–
N-DOPE-NBD	di(14:1)PC	2.9	–
(18:1-(12:0-NBD))-PE	di(18:1)PC	2.0	1.0
(18:1-(12:0-NBD))-PC	di(18:1)PC	2.0	1.0
(18:1-(12:0-NBD))-PG	di(18:1)PC	2.3	1.1
(18:1-(12:0-NBD))-PS	di(18:1)PC	2.7	1.3
(18:1-(12:0-NBD))-PA	di(18:1)PC	3.0	1.5

Reprinted with permission from (10). Copyright 2004 Biophysical Society
[a] $K_S(PC)$ is the relative association constant of (18:1-(12:0-NBD))-PC

Figure 3 shows the FRET efficiencies measured between the Trp151 in LacY protein and either Pyr-PG or Pyr-PE as acceptors in the different lipid systems at 37 °C, together with the theoretical values, calculated using different values for the probability of finding a given phospholipid in the annular region (μ). Higher FRET efficiencies are obtained for transfer to Pyr-PE compared to Pyr-PG in both POPE/POPG and DOPE/POPG proteoliposomes, reflecting preferential interaction for PE in both systems. Application of the selectivity model described above to the experimental values indicates that PE concentration in the protein-annular region is approximately ~86 mol% for DOPE/POPG ($\mu(PE) = 0.86$, $\mu(PG) = 0.14$), and 100 % for POPE/POPG ($\mu(PE) = 1.00$, $\mu(PG) = 0.00$), whereas 75 mol% would be expected for a random distribution of both phospholipids. For proteoliposomes composed of DPPE/POPG with POPG-enriched fluid domains coexisting with DPPE-enriched gel-phase bilayer regions, an increase in the efficiency of FRET to Pyr-PG and a decrease in that to Pyr-PE are verified (Fig. 3), to an extent that the efficiency of FRET to Pyr-PG now clearly surpasses that to Pyr-PE. This result indicates that the protein is preferentially located in fluid domains where Pyr-PG is more abundant than Pyr-PE.

In order to test for the effects of cardiolipin (CL) in the annular region of LacY, myristoyl-CL and oleoyl-CL were incorporated in the POPE/POPG proteoliposomes. Addition of CL resulted always in a decrease of FRET efficiencies (Table 2) reflecting displacement of POPE and POPG lipids from the annular region of the protein. The effect was more significant when

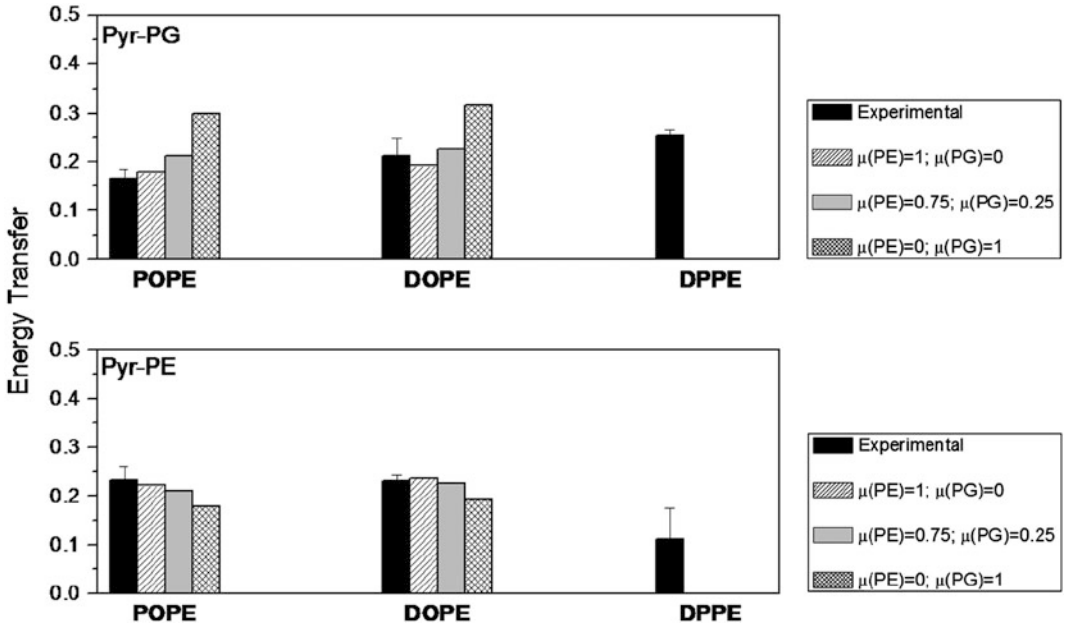

Fig. 3. Comparison of experimental and theoretical values of FRET efficiency between W151 and Pyr-PG (*top*) and Pyr-PE (*bottom*) at 37 °C in POPE:POPG (3:1, mol/mol) (*left*), DOPE:POPG (3:1, mol/mol) (*center*), and DPPE:POPG (3:1, mol/mol) (*right*) proteoliposomes (1.5 μM LacY). Reprinted with permission from (14). Copyright 2010 Elsevier.

Pyr-PG was used as the acceptor, likely due to the preference of the protein for PE species as described above. In fact, when the acceptor is Pyr-PG, even by imposing segregation of this probe from the first annular layer ($\mu(PG) = 0$) in the FRET quantitative model, it is not possible to conciliate the theoretical (0.162) and the experimental values (0.143 for oleoyl-CL, 0.142 for myristoyl-CL); see Table 2. This is an indication that the changes in lateral lipid distribution induced by the presence of the protein extend beyond the first layer of lipids around it, as PG is still somewhat rarefied in this area. On the other hand, when A is Pyr-PE, a model matching to the experimental efficiencies (0.183 for oleo CL, 0.196 for myristoyl-CL) requires only partial replacement of PE by CL. When the CL lipid is oleoyl-CL, the retrieved composition of the annular layer is 40 mol% PE and 60 mol% CL. On the other hand, when the CL lipid is myristoyl-CL, the composition of the annular layer is 68 mol% PE and 32 mol% CL, indicating that in this case PE is kept in close proximity of the protein, in the same proportion as in the bulk. In fact, upon addition of myristoyl-CL to the system, CL enrichment around the protein is solely produced by replacing PG molecules. Unlike oleoyl-CL, myristoyl-CL is not able to displace PE from the area around the protein, probably due to the hydrophobic mismatch between the short myristoyl acyl chains and the protein.

Table 2
Comparison of experimental and theoretical FRET efficiencies between LacY W151 and Pyr-PE or Pyr-PG acceptors, for ternary mixtures PE:PG:CL 67:23:10 at 37°C

Lipid composition	Experimental	μ(PE) = 0.67, μ(PG) = 0.23, μ(CL) = 0.10 (all random)	Best fit	Parameter set for composition of first layer
67 POPE:22.75 POPG:10 oleo CL:0.25 Pyr-PG	$E = 0.1434$	$E = 0.1960$	$E = 0.1621$ (μ(PG) = 0.00)	μ(PE) = 0.40, μ(PG) = 0.00, μ(CL) = 0.60
66.75 POPE:23 POPG:10 oleo CL:0.25 Pyr-PE	$E = 0.1826$	$E = 0.1960$	$E = 0.1826$ (μ(PE) = 0.40)	
67 POPE:22.75 POPG:10 myr CL:0.25 Pyr-PG	$E = 0.1423$	$E = 0.1960$	$E = 0.1621$ (μ(PG) = 0.00)	μ(PE) = 0.68, μ(PG) = 0.00, μ(CL) = 0.32
66.75 POPE:23 POPG:10 myr CL:0.25 Pyr-PE	$E = 0.1963$	$E = 0.1960$	$E = 0.1964$ (μ(PE) = 0.68)	

Reprinted with permission from (14). Copyright 2010 Elsevier

4. Notes

1. In the examples that illustrate this chapter, one-component systems (DOPC, DEuPC, DMoPC) were addressed in the DCIA-M13 mcp system, whereas two- (POPE/POPG, DOPE/POPG, DPPE/POPG; 3:1 in all cases) and three-component (POPE/POPG/oleoyl-CL and POPE/POPG/myristoyl-CL, 67:23:10 in both cases) mixtures were explored in the LacY system.
2. The amount of added acceptor is somewhat arbitrary, but affected by the R_0 value. Lower R_0 values may require higher amounts of acceptor. In the examples that illustrate this chapter, acceptor concentration was varied between ~0.1 and 2.5 mol% of total lipid in the DCIA-M13 mcp system (for the DCIA/NBD FRET pair, $R_0 = 3.9$ nm) and fixed at 0.25 mol% in the LacY system (for the LacY/Pyr FRET pair, $R_0 = 3.0$ nm). Very high acceptor concentrations are not advised, as in these circumstances, FRET to non-bound A molecules dominates over the annular FRET component, rendering recovery of K_s or μ more difficult.

3. In the examples that illustrate this chapter, DCIA M13 mcp was reconstituted by a dialysis procedure. Lipid vesicles were mixed with the wild-type and labeled protein. Dialysis was carried out at room temperature and in the dark, with a 100-fold excess of buffer II, which was replaced five times every 12 h. On the other hand, for LacY reconstitution, lipid vesicle suspensions containing 0.2 % of DDM were incubated overnight at room temperature. Liposomes were subsequently mixed with the solubilized protein and incubated at 4°C for 30 min, with gentle agitation. DDM was extracted by addition of Bio-Beads SM-2.
4. This FRET methodology requires accurate knowledge of acceptor concentrations. It is therefore advisable to conduct a spectrophotometric determination of acceptor concentration and a quantification of phospholipid content (through the analysis of inorganic phosphate) after the reconstitution procedure. This is particularly important in case dialysis was performed, as a significant amount of material is lost during the procedure. Additionally, FRET measurements based on donor steady-state fluorescence intensities are more prone to error due to variability in donor concentration between different samples. Fluorescence lifetime measurements circumvent this problem as they are independent of concentration.
5. In the frequent case of multiexponentially decaying D, fluorescence lifetimes are replaced in Eq. 3 by the amplitude-weighted mean lifetime (15), defined by

$$\overline{\tau} = \sum_{i=1}^{m} \alpha_i \tau_i, \tag{11}$$

where α_i and τ_i are the normalized amplitudes and lifetime values of the $m > 1$ components necessary for a statistically adequate description of the D decay (either in absence or in presence of acceptor).
6. Typical values for the refractive index n and the orientation factor κ^2 are 1.4 (16) and 2/3 (dynamic isotropic limit, good approximation in fluid bilayers; see (17) for a discussion), respectively.
7. In the examples that illustrate this chapter, area per lipid was taken as 0.72 nm^2 for the host lipids used in the DCIA M13 mcp system, and 0.56, 0.56, and 1.26 nm^2 for POPE, POPG, and CL, respectively, in the LacY system. As for the interplanar distances, in the DCIA M13 system, the D chromophore was known to reside in the bilayer midplane (18), and $l_1 = l_2$ values were 1.89, 1.98, 1.54, and 2.24 nm for *N*-NBD-DOPE in DOPC, all NBD acyl chain lipids in DOPC, *N*-NBD-DOPE in DMoOPC, and *N*-NBD-DOPE in DEuPC, respectively.

On the other hand, for the LacY system, it was assumed that the A chromophore (pyrene in acyl-chained labeled lipids) was located in the center of the bilayer, and $l_1 = l_2 = 1.2$ nm was considered. The number of annular sites was $N = 12$ for DCIA M13 mcp and $N = 46$ for LacY.

8. If the host lipid matrix is a mixture of two or more components, then the meaning of K_s is not so well defined, as in this instance it becomes dependent on the particular composition of the lipid mixture. For this reason, in the LacY case example, no K_s values are retrieved, and only μ is calculated for each system.

Acknowledgments

F.F. acknowledges a research grant (SFRH/BPD/64320/2009) from Fundacão para a Ciência e Tecnologia (FCT). F.F., M.P., and L.M.S.L. acknowledge funding by FEDER (COMPETE program), and by FCT (Fundação para a Ciência e a Tecnologia), project references PTDC/QUI-BIQ/112067/2009, PTDC/QUI-BIQ/099947/2008, and FCOMP-01-0124-FEDER-010787 (FCT PTDC/QUI-QUI/098198/2008).

References

1. Marsh D (2008) Electron spin resonance in membrane research: protein-lipid interactions. Methods 46:83–96
2. Nyholm TK, Ozdirekcan S, Killian JA (2007) How protein transmembrane segments sense the lipid environment. Biochemistry 46:1457–1465
3. Czech MP (2000) PIP2 and PIP3: complex roles at the cell surface. Cell 100:603–606
4. Lee AG (2003) Lipid–protein interactions in biological membranes: a structural perspective. Biochim Biophys Acta 1612:1–40
5. Marsh D, Horváth LI (1998) Structure, dynamics and composition of the lipid–protein interface. Perspectives from spin-labeling. Biochim Biophys Acta 1376:267–296
6. London E, Feigenson GW (1981) Fluorescence quenching in model membranes. 1. Characterization of quenching by a spin-labeled phospholipid. Biochemistry 20:1932–1938
7. Everett J, Zlotnick A, Tennyson J, Holloway PW (1986) Fluorescence quenching of cytochrome b5 in vesicles with an asymmetric transbilayer distribution of brominated phosphatidylcholine. J Biol Chem 261:6725–6729
8. Förster T (1949) Experimentelle und theoretische Untersuchung des Zwischenmolekularen übergangs von Elektrinenanregungsenergie. Z Naturforsch 4a:321–327
9. Van Der Meer B, Coker V III, Chen S-YS (1994) Resonance energy transfer: theory and data. VCH Publishers, New York
10. Fernandes F, Loura LMS, Koehorst R, Spruijt RB, Hemminga MA, Fedorov A, Prieto M (2004) Quantification of protein-lipid selectivity using FRET: application to the M13 major coat protein. Biophys J 87:344–352
11. Fung BK, Stryer L (1978) Surface density determination in membranes by fluorescence energy transfer. Biochemistry 17:5241–5248
12. Wolber PK, Hudson BS (1979) An analytical solution to the Förster energy transfer problem in two dimensions. Biophys J 28:197–210
13. Spruijt RB, Wolfs CJ, Verver JW, Hemminga MA (1996) Accessibility and environment probing using cysteine residues introduced along the putative transmembrane domain of

the major coat protein of bacteriophage M13. Biochemistry 35:10383–10391

14. Picas L, Suárez-Germà C, Montero MT, Vázquez-Ibar JL, Hernández-Borrell J, Prieto M, Loura LM (2010) Lactose permease lipid selectivity using Förster resonance energy transfer. Biochim Biophys Acta 1798:1707–1713
15. Lakowicz JR (2006) Principles of fluorescence spectroscopy, 3rd edn. Kluwer Academic/Plenum, New York
16. Davenport L et al (1985) Transverse location of the fluorescent probe 1,6-diphenyl-1,3,5-hexatriene in model lipid bilayer membrane systems by resonance energy transfer. Biochemistry 24:4097–4108
17. Loura LMS, Fedorov A, Prieto M (1996) Resonance energy transfer in a model system of membranes: application to gel and liquid crystalline phases. Biophys J 71:1823–1836
18. Koehorst RBM, Spruijt RB, Vergeldt FJ, Hemminga MA (2004) Lipid bilayer topology of the transmembrane α-helix of M13 major coat protein and bilayer polarity profile by site-directed fluorescence spectroscopy. Biophys J 87:1445–1455.